

Hydrogen bonded networks in formamide [HCONH₂]_n ($n = 1 - 10$) clusters: A computational exploration of preferred aggregation patterns[#]

A SUBHA MAHADEVI, Y INDRA NEELA and G NARAHARI SASTRY*

Molecular Modeling Group, Indian Institute of Chemical Technology, Tarnaka, Hyderabad 500 607, India
e-mail: gnsastry@gmail.com

Abstract. Application of quantum chemical calculations is vital in understanding hydrogen bonding observed in formamide clusters, a prototype model for motifs found in protein secondary structure. DFT calculations have been performed on four arrangements of formamide clusters [HCONH₂]_n, ($n = 1 - 10$) linear, circular, helical and stacked forms. These studies reveal the maximum cooperativity in the stacked arrangement followed by the circular, helical and linear arrangements and is based on interaction energy per monomer. In all these arrangements as we increase cluster size, an increasing trend in cooperativity of hydrogen bonding is observed. Atoms-in-molecule analysis establishes the nature of bonding between the formamide monomers on the basis of electron density values obtained at the bond critical point (BCP).

Keywords. Cooperativity; hydrogen bonding; AIM analysis; N–H stretching frequency.

1. Introduction

The study of molecular clusters has become a topic of outstanding contemporary interest. Understanding the nature of interactions in molecular clusters is particularly relevant to furthering our knowledge on supramolecular architecture and stability. The bottom up approach of building large assemblies from constituent monomers has found extensive favour in the field of nanomaterial science.¹ A large number of theoretical studies have been performed on diverse supramolecular assemblies including clusters of argon², CO₂³, benzene⁴, etc.

Among molecular clusters, hydrogen bonded molecular clusters have been the focus of substantial amount of attention in particular the water molecule.⁵ Extensive *ab initio* calculations have been performed for several possible structures of water clusters (H₂O)_n, $n = 8 - 20$. These studies reveal how most stable geometries seem to arise from a fusion of tetrameric or pentameric rings.⁶ Phenol, water and phenol–water clusters have been used to demonstrate the contribution of hydrogen bonding to their structure and stability and is based on *ab initio* and DFT calculations and uses topological features of electron density.⁷ Studies at HF, B3LYP and MP2 level of theory on helical $n = 5 - 20$ ⁸ and also on spirocyclic arrangements⁹ have demonstrated the multitude of variation possible in

structure when one deals with water clusters. Our study on four different arrangements of water clusters including W1D, W2D, W2D–helical and the caged clusters from Cambridge cluster database $n = 2 - 20$ has shown how the cooperativity observed in hydrogen bonding is dependant to a large extent on type of arrangement of water molecules.¹⁰ This study also addresses the structural and energetic preferences of anion and cation radicals of water clusters in comparison to the neutral clusters. The role of polarity of the environment and how this determines the stability of water cluster has also been explored using theoretical studies.¹¹ Thus, water clusters are the best studied model systems of hydrogen bonding. The primary interactions seen in these clusters are non covalent interactions.¹² Systematic studies on the strength of non covalent interactions and role of the size of molecules have been reported.¹³ The study of the non bonded interactions including cation — π and $\pi - \pi$ interactions and their dependence on solvent also has been extensively investigated.¹⁴

Several other molecular clusters have also been the subject of theoretical calculations.¹⁵ High level *ab initio* calculations have been used to investigate cooperative aspects of C–H...N H–bonding in (HCN)_n, $n = 1-7$ clusters on the basis of energetic, structural and vibrational properties.¹⁶ Large cooperativity in N–methylacetamide clusters ($n = 1-5$) has been demonstrated based on geometries, chemical shifts as well as quadrupole coupling values for each species using DFT calculations involving quantum cluster equilibrium methodology.¹⁷ Another interesting

[#]Dedicated to Prof. N Sathyamurthy on his 60th birthday

*For correspondence

theoretical investigation compares how CH...O hydrogen bonds compare to their more classical OH...O or OH...N analogues in terms of cooperativity and this has been demonstrated by comparing $(\text{H}_2\text{CO})_n$ cluster as well as $(\text{HFCO})_n$ clusters with water clusters.¹⁸ Nanotube and nanoring forms of boric acid forms, structurally similar to carbon nanotubes, with extensive hydrogen-bonding network have been designed based on *ab initio* calculations using the cardinality guided molecular tailoring approach.¹⁹ These studies have revealed how the stability of these tubes increase as the diameter increases due to the enhancement in the number of H-bonding interactions. Several other studies on crystals of acetic acid,²⁰ urea,²¹ nitroanilines²², etc. have also been employed to understand hydrogen bonding. Several non-covalent interactions including hydrogen bonding have a mutually enhancing effect over each other. This phenomenon of cooperativity among two non-bonded interactions has been widely explored.²³ There have been several reports of theoretical studies on cooperative H-bonding in amides including formamide and acetamide involving small number of molecules.²⁴ Dannenberg *et al.* have clearly elucidated cooperativity in hydrogen bonded formamide chains of length up to $n = 15$ using B3LYP/D95** level of theory.²⁵ They explain the significance of cooperativity in the context of understanding its relevance in protein structure modelling. Thus, hydrogen bonding in molecular clusters and the manifestation of its cooperative behaviour continue to be a topic of high current interest. In a recent study we have investigated the extent of cooperativity in hydrogen bonding in different kinds of arrangements of acetamide clusters $n = 1-15$.²⁶

In the present study, we seek to understand the relevance of arrangement of individual monomers; in clusters of formamide and its impact on the extent of hydrogen bonding that is manifested as a consequence. Although several important theoretical studies on formamide clusters exist^{24,25}, quantum chemical calculations on impact of variation in spatial arrangement of formamide clusters have not been attempted. We undertake this study to essentially quantify the amount of cooperativity that is known to exist in formamide clusters of size 1-10 as a function of arrangement of clusters.

2. Methodology

Geometry optimizations are performed at B3LYP/D95** level of theory in gas phase for four arrangements of formamide clusters (linear, circular,

helical and stacked), $n = 1 - 10$ without any constraints. Frequency calculations were done to ascertain nature of stationary points obtained for all the optimized geometries. The frequencies reported here have not been modified by any scaling factor. The interaction energy (IE in kcal/mol) for each cluster is calculated as shown below.

$$IE = E_{\text{total}} - n * E_{\text{monomer}}, \quad (1)$$

E_{total} – Total energy of cluster, E_{monomer} – Total energy of a single molecule, n – number of monomers.

The interaction energy per hydrogen bond (IE/HB) and more importantly per monomer (IE/n) for each cluster is calculated, in order to indicate change in strength of hydrogen bond with increasing cluster size, and as a measure to quantify cooperativity in the clusters. The interaction energies were then corrected for basis set superposition error (BSSE) using the counterpoise method established by Boys and Bernardi.²⁷ Further single point calculations on these optimized geometries were performed at B3LYP/cc-pVTZ level of theory along with corresponding BSSE calculations at the same level. All the above mentioned calculations were carried out using the Gaussian 03 program.²⁸ In order to evaluate the nature of hydrogen bonding interactions, topological analysis of the electron density distribution within Bader's atoms in molecules theory (AIM) was performed.²⁹ The total electron density $\rho(\mathbf{r})$ is calculated from the wave function of the equilibrium geometry of the various clusters at B3LYP/D95** level. The bond critical points (3, -1) are then characterized by a rank of 3 and a signature of -1.

3. Results and discussion

This section gives an overview of the structure and energetics of the four arrangements of the formamide clusters. This is followed by an evaluation of the cooperativity seen in them and its correlation with results of AIM analysis.

3.1 Interaction energy and cooperativity

The B3LYP/D95** optimized geometries of $n = 2$ and $n = 10$ clusters of formamide in four arrangements are shown in figure 1. The optimized geometries of all the remaining structures considered in the present study are provided in the supporting information. All the optimized clusters are found to be minima on the potential energy surface. Among the four arrangements

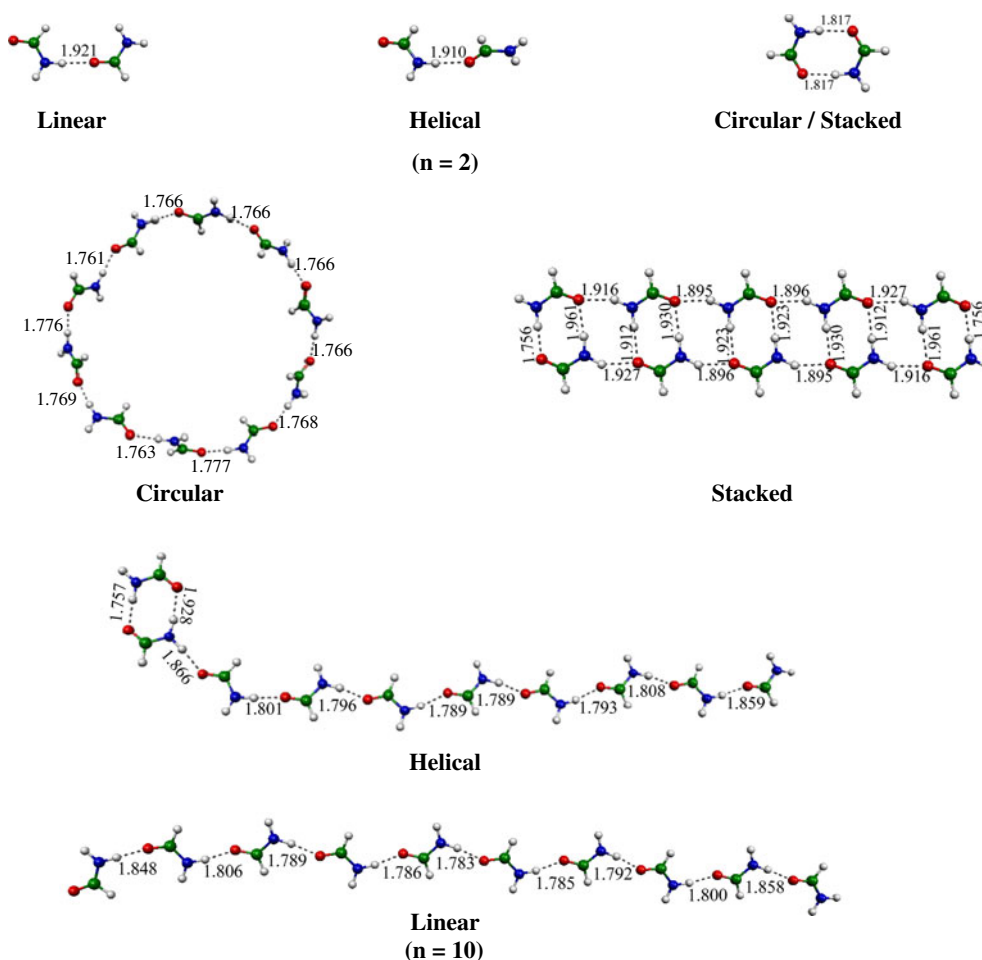


Figure 1. Optimized geometries of four arrangements of formamide clusters ($n = 2$ and 10) at B3LYP/D95** level of theory. O--H bond distances are in Å.

considered in the present study the clusters have C_1 symmetry except the stacked form.

The BSSE corrected interaction energy of these clusters at B3LYP/D95** level and B3LYP/cc-pVTZ level as a function of cluster size all shown in figure 2(a). For a cluster of a given size, the highest interaction energy is observed in the stacked arrangement followed by the circular, helical and linear arrangements, respectively. The magnitude of this interaction energy at B3LYP/D95** is as follows for $n = 2 - 10$ clusters; linear (-5.88 to -75.52 kcal/mol), circular (-14.00 to -91.48 kcal/mol), helical (-6.36 to -79.50 kcal/mol) and stacked (-14.00 to -108.9 kcal/mol). The graph shows high similarity between linear and helical forms for $n = 2 - 4$ arrangements in terms of interaction energy. This trend is retained to a large extent in case of clusters of size $n = 5 - 10$, although slightly higher (~ 5 kcal/mol) IE is seen in the helical arrangement. A similar comparison can be made between the stacked and circular arrangements. However, for clusters of size $n = 6 - 10$, slightly higher ($\sim 8 - 18$ kcal/mol)

IE are seen in the stacked arrangement. Figure 2(b) provides important information on interaction energy per monomer (IE/n in kcal/mol). It gives an indication of how addition of one more monomer entity to the cluster affects its interaction energy in the context of a particular kind of arrangement. The trend for IE/n values is stacked $>$ circular $>$ helical $>$ linear arrangements. An important observation is the steady increase in IE/n for all the arrangements. However, subtle variations do exist in the extent of increase in IE/n when we consider the different arrangements of the clusters. The linear arrangement has IE/n values ranging between -2.94 and -7.55 kcal/mol. There is a greater impact of addition of monomer to the linear cluster, for size $n = 2 - 6$ as the increase in IE/n is between 0.5 and 1.5 kcal/mol for every monomer added. From $n = 7$ onward a minor increase in IE/n of ~ 0.2 kcal/mol is noted. In the case of the helical arrangement a similar trend is noted with the IE/n values which plateau out from $n = 5$ onwards with a very small increase of ~ 0.2 kcal/mol on the addition

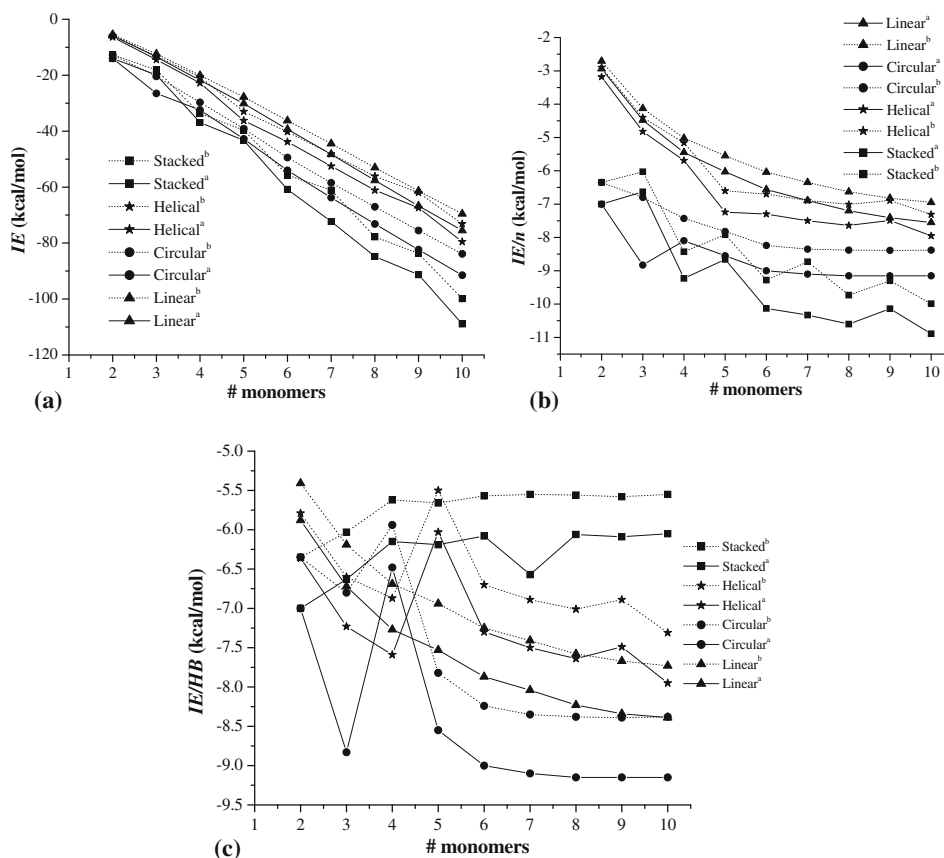


Figure 2. Plot of BSSE corrected (a) Interaction energy (IE). (b) Interaction energy per monomer, (IE/n) and (c) Interaction energy per hydrogen bond, (IE/HB) in kcal/mol versus number of monomers in four arrangements of formamide clusters, $n = 2 - 10$ optimized at B3LYP/D95** level of theory. ^aSolid lines indicate values at B3LYP/D95** level of theory; ^bdotted lines indicate values at B3LYP/cc-pVTZ level of theory.

of each monomer. The range of IE/n for cluster sizes $n = 2 - 10$ of the circular arrangement is comparatively narrow (-7.00 to -9.15 kcal/mol). From $n = 6$ onward barely any increase in IE/n (< 0.1 kcal/mol) is noted. The even numbered stacked clusters ($n = 2, 4, 6, 8$ and 10) have higher IE/n compared to the odd numbered clusters ($n = 3, 5, 7$ and 9). This presents a more uneven increase in IE/n as cluster size increases. The range of IE/n for cluster sizes $n = 2 - 10$ in case of the stacked arrangement is -7.0 to -10.89 kcal/mol. Although the trend for IE/n and IE/HB are similar for linear, helical and circular clusters for $n = 5$ onward, a surprisingly flat pattern is noted in case of stacked clusters for IE/HB as is seen in figure 2(c). Apparently there is no change in IE/HB as the cluster size increases in the stacked arrangement. Table S1 of the supporting information thus clearly reveals the impact of basis set superposition error in these calculations (between 0.99 and 1.50 kcal/mol for $n = 2$ while much higher impact is noticed for $n = 10$;

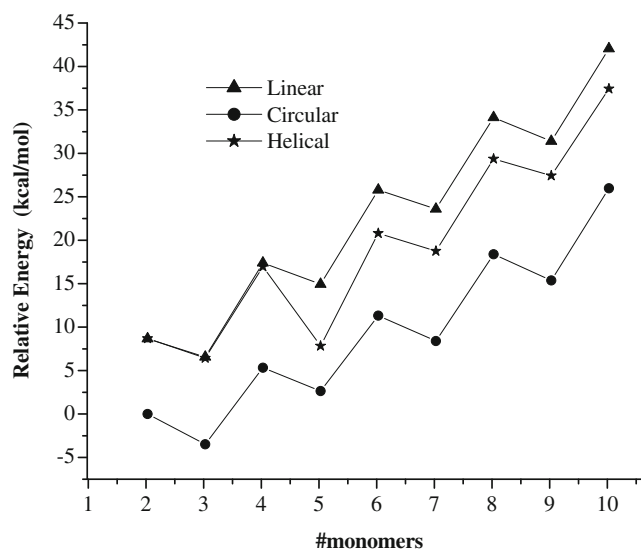


Figure 3. Plot of relative energy of linear, circular and helical arrangement with respect to the stacked form versus number of monomers of formamide clusters, $n = 2 - 10$ at B3LYP/D95** level of theory.

Table 1. Average O--H bond length (in Å) for formamide clusters $n = (2 - 10)$ calculated at B3LYP/D95** level of theory.

n	Linear	Circular	Helical	Stacked
2	1.921	1.817	1.910	1.817
3	1.876	1.806	1.882	1.861
4	1.853	1.892	1.743	1.888
5	1.836	1.712	1.874	1.892
6	1.828	1.665	1.841	1.897
7	1.820	1.665	1.834	1.832
8	1.816	1.768	1.828	1.900
9	1.814	1.768	1.819	1.851
10	1.805	1.768	1.819	1.905

between 11.5 and 20.5 kcal/mol) for all the different arrangements as a function of increasing size of the system. The extent of impact of BSSE correction in case of formamide clusters is also higher when the D95** basis set is employed compared to the cc-pVTZ basis set.

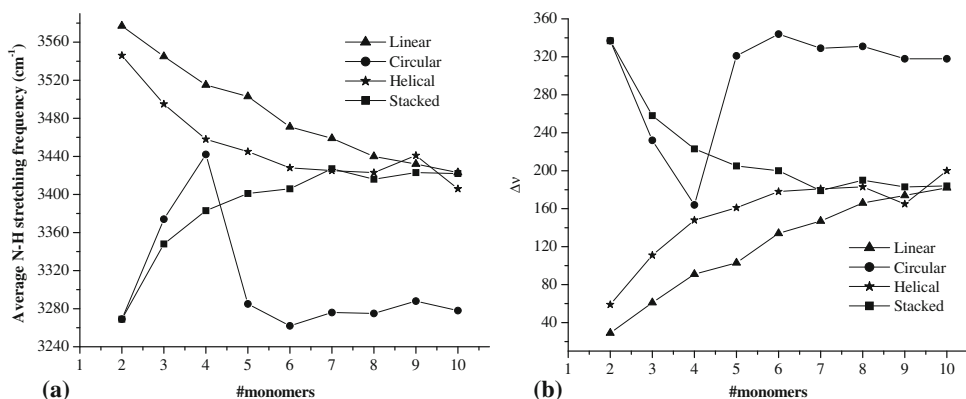
Figure 3 also demonstrates the greater stability of the stacked arrangement compared to circular, helical or linear forms as it plots the relative energy of the above mentioned three forms with respect to the total energy of a stacked cluster of the same size. The preceding discussion on the energetics of the formamide clusters helps to reinforce the concept of cooperativity, where addition of one more monomer to the cluster enhances the strength of the hydrogen bond interaction among individual monomer units. This seems to hold good for all the arrangements which we have considered as part of our study, and clearly the mode of arrangement determines to a great deal the extent of cooperativity which is demonstrated.

3.2 Optimized geometries

The O--H bond distances in Å for the four arrangements we have studied are shown in table 1. Considering the O--H bond distances, both the linear and helical arrangements show longer bond distances toward the termini while towards the central portion of the chain the O--H bond distance is shorter. The stacked arrangements have lower O--H bond distance values (~ 1.740 Å) towards the outer hydrogen bonds compared to more interior located ones (~ 1.920 Å). In contrast, the circular arrangements show more uniform O--H bond distance values. In three of these arrangements a definite shortening of the O--H hydrogen bond is observed as we increase the cluster size from 2 to 10 (linear: 1.921 to 1.805 Å; circular: 1.817 to 1.768 Å; helical: 1.910 to 1.819 Å). This shortening trend for O--H bond distance is not noted when the stacked clusters are considered even though the interaction energy per monomer is highest amongst them. The greater symmetry in arrangement of these clusters along with closer packing of the monomers leads to maximizing the number of interactions in them. This in turn may be responsible for the flat pattern in IE/HB noted in case of stacked clusters.

3.3 N-H stretching frequencies

Vibrational frequency shifts are used as a measure to gauge the cooperative nature of H-bonding interactions.²⁵ In the case of clusters where H-bonding interaction is manifested, N-H stretching frequency shifts to a lower value and its intensity increases. The extent of decrease in N-H stretching frequency depends on

**Figure 4.** Plot of (a) average N-H stretching frequency versus number of monomers and (b) deviation in average N-H stretching frequency from monomer stretching frequency in four arrangements of formamide clusters, $n = 2 - 10$ at B3LYP/D95** level of theory.

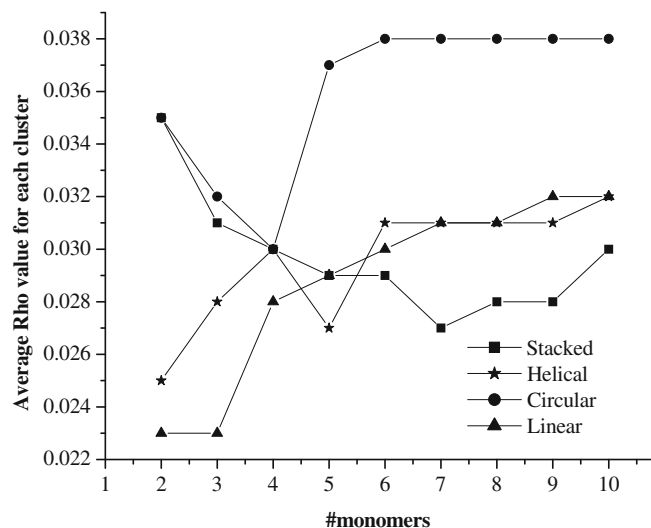


Figure 5. Plot of average ρ value of cluster versus number of monomers in four arrangements of formamide clusters, $n = 2 - 10$ at B3LYP/D95** level of theory.

the strength of H-bonding interaction. We compared the magnitude of shift in N–H stretching frequency in each arrangement to demonstrate the variation in cooperativity among different arrangements. This is done using

two parameters, average N–H stretching frequency value for each cluster and deviation of average N–H stretching value from that computed for a monomer ($\Delta\nu$). For the isolated formamide molecule, the $\nu_{\text{N-H}}$ frequency is detected at 3606 cm^{-1} . Figure 4 presents graphical plots of the above mentioned two parameters versus the cluster size calculated at B3LYP/D95** level of theory. A marked red shift is observed in case of linear and stacked arrangements as the cluster size increases from $n = 2 - 10$. While both helical and linear forms show average frequency value between ($3546 - 3406 \text{ cm}^{-1}$) and ($3577 - 3423 \text{ cm}^{-1}$), respectively, they also have a steady increase in $\Delta\nu$ which is a convenient measure of harmonic frequency cooperativity. The circular clusters have average frequency values much lower compared to the monomer indicating a definite red shift. From $n = 5$ onwards all circular clusters up to size $n = 10$ have average N–H stretching values ranging between 3260 and 3288 cm^{-1} . This is seen in the graph as a flat portion in case of the circular arrangement. The stacked conformations behave differently in this context. The highest deviation of average N–H stretching frequency value for each cluster from that of a monomer is seen for $n = 2$ cluster. As the cluster size increases this deviation value decreases, uniquely

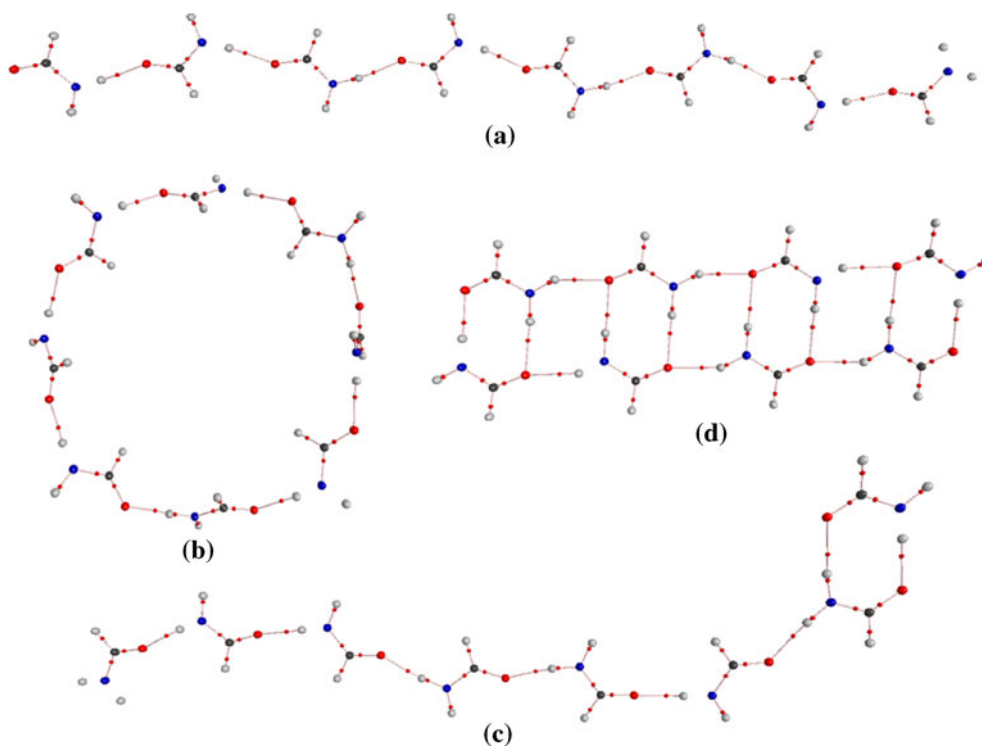


Figure 6. AIM analysis on B3LYP/D95** optimized geometries of ($n = 8$) (a) Linear (b) Circular (c) Helical and (d) Stacked) formamide clusters. Line joining atoms indicate bond path as calculated using AIM2000.

in the stacked arrangement. Thus N–H stretching frequencies have been employed as an effective measure of harmonic frequency cooperativity.

3.4 AIM analysis

In order to characterize the hydrogen bonding interaction between two formamide monomers, the electron density at bond critical points was taken into account. According to AIM theory, any chemical bond including hydrogen bonding is characterized by the presence of so-called bond critical points (BCP). The bond critical points (3, –1) are characterized by a rank of 3 and a signature of –1. This means that the electron density at this point has a minimal value along the line of the bond and a maximal value in two orthogonal directions.

Figure 5 gives a picture of how cluster size and different spatial arrangements impact average electron density (ρ) of a formamide cluster. The linear, helical and circular arrangements show an increase in average ρ value as cluster size increases. The maximum average ρ values are observed in the circular structures even though from $n = 5$ onwards they are uniformly around 0.038 a.u. The linear and helical forms show average ρ values ranging between 0.023 and 0.032 a.u. as the cluster size progresses from $n = 2 - 10$. This kind of uniformity is not observed in the stacked arrangement and decreasing average ρ values with increasing cluster size are found with respect to these cluster arrangements. Figure 6 shows the molecular topographs of selected formamide clusters ($n = 8$) for the different arrangements. A point to be noted with regard to the linear and helical forms is the higher values of ρ at the BCP of the central hydrogen bonds when compared to the termini correlating with their shorter O–H bond lengths.

4. Conclusions

The structure and energetics of four different arrangements of formamide clusters ($n = 2 - 10$) at B3LYP/D95** level of theory have been explored. On the basis of total energy, the relative stability of the stacked form in comparison to the other three forms is established. We find a clear manifestation of cooperativity in hydrogen bonding in all the cluster forms as evidenced by the corresponding increase in interaction energy per monomer with an increase in cluster size. A significant impact of BSSE is noted in the calculations with the increase in the size of cluster. The decrease in value of average N–H stretching frequencies leading to a red shift in larger clusters correlates to the enhanced

hydrogen bonding and is used to explain cooperativity. Higher average ρ values obtained by AIM analysis help to establish the nature of hydrogen bonding in the formamide clusters. Thus, the mode of arrangement of monomers in all the cluster forms determines to a great deal the extent of cooperativity observed.

Supporting information

Table of interaction energy (IE in kcal/mol) along with optimized geometries of all arrangements at B3LYP/D95** level, O–H bond distances between two monomers in all the clusters, all the N–H stretching frequencies observed for each cluster and pictorial representation of AIM analysis of all clusters is provided in the supporting information (tables S1-S3 and figures S1-S8). See www.ias.ac.in/chemsci for supporting information.

Acknowledgements

The Department of Science and Technology (DST) is thanked for Swarnajayanthi Fellowship to GNS, Woman Scientist Scheme (WOS–A) to ASM, and INSPIRE Fellowship to YIN. The financial support received from Department of Atomic Energy–Board of Research in Nuclear Sciences, Mumbai to GNS is also acknowledged.

References

1. (a) Hoeben F J M, Jonkheijm P, Meijer E W and Schenning A P H J 2005 *Chem. Rev.* **105** 1491 (b) Cañas-Ventura M E, Ait–Mansour K, Ruffieux P, Reiger R, Müllen K, Brune H and Fasel R 2010 *ACS Nano* **5** 457 (c) Elango M, Parthasarathi R, Subramanian V, Ramachandran C N and Sathyamurthy N 2005 *Proc. Indian Natl. Sci. Acad.* **71A** 405
2. Rusek M and Orłowski A 2004 *Acta Phys. Pol.* **A106**
3. Takeuchi H J 2008 *Phys. Chem.* **A112** 7492
4. Mahadevi A S, Rahalkar A P, Gadre S R and Sastry G N 2010 *J. Chem. Phys.* **133** 164308
5. (a) Parthasarathi R, Subramanian V and Sathyamurthy N 2008 *Syn. React. Inor. Metal–Org. Nano–Metal Chem.* **38** 18 (b) Elango M, Parthasarathi R, Subramanian V, Ramachandran C N and Sathyamurthy N 2006 *J. Phys. Chem. A* **110** 6294 (c) Parthasarathi R, Subramanian V, Sathyamurthy N and Leszczynski J 2007 *J. Phys. Chem.* **A111** 2 (d) Parthasarathi R, Subramanian V and Sathyamurthy N 2007 *J. Phys. Chem.* **A111** 13287 (e) Suhai S 1996 *J. Phys. Chem.* **100** 3950 (f) Suhai S 1995 *J. Chem. Phys.* **103** 7030
6. Maheshwary S, Patel P, Sathyamurthy N, Kulkarni A D and Gadre S R 2001 *J. Phys. Chem.* **A105** 10525
7. Parthasarathi R, Subramanian V and Sathyamurthy N 2005 *J. Phys. Chem.* **A109** 843

8. Parthasarathi R, Elango M, Subramanian V and Sathyamurthy N 2009 *J. Phys. Chem.* **A113** 3744
9. Elango M, Subramanian V and Sathyamurthy N 2009 *J. Chem. Sci.* **121** 839
10. Neela Y I, Mahadevi A S and Sastry G N 2010 *J. Phys. Chem.* **B114** 17162
11. Ramachandran C N and Sathyamurthy N 2005 *Chem. Phys. Lett.* **410** 348
12. (a) Dougherty D A 1996 *Science* **271** 163 (b) Ma J C and Dougherty D A 1997 *Chem. Rev.* **97** 1302 (c) Reddy A S and Sastry G N 2005 *J. Phys. Chem.* **A109** 8893 (d) Reddy A S, Sastry G M and Sastry G N 2007 *Proteins Struct. Funct. Bioinf.* **67** 1179 (e) Nagaraju M and Sastry G N 2009 *Int. J. Quant. Chem.* **110** 1994 (f) Mahadevi A S and Sastry G N 2010 *J. Phys. Chem.* **B115** 703
13. (a) Vijay D and Sastry G N 2008 *Phys. Chem. Chem. Phys.* **10** 582 (b) Priyakumar U D, Punnagai M, Krishna Mohan G P and Sastry G N 2004 *Tetrahedron* **60** 3037 (c) Priyakumar U D, Reddy A S and Sastry G N 2004 *Tet. Lett.* **45** 2495
14. (a) Reddy A S, Zipse H and Sastry G N 2007 *J. Phys. Chem.* **B111** 11546 (b) Rao J S, Zipse H and Sastry G N 2009 *J. Phys. Chem.* **B113** 7225 (c) Vijay D and Sastry G N 2006 *J. Phys. Chem.* **B 110** 10148 (d) Rao J S, Dinadayalane T C, Leszczynski J and Sastry G N 2008 *J. Phys. Chem. A* **112** 12944
15. (a) Guo H, Gresh N, Roques B P and Salahub D R 2000 *J. Phys. Chem.* **B104** 9746 (b) Ludwig R 2000 *J. Mol. Liq.* **84** 65
16. King B F, Farrer T C and Weinhold F 1995 *J. Chem. Phys.* **103** 348
17. Ludwig R, Weinhold F and Farrar T C 1997 *J. Phys. Chem.* **A101** 8861
18. Karr T and Scheiner S 2004 *J. Phys. Chem.* **A108** 9161
19. (a) Elango M, Subramanian V, Rahalkar A P, Gadre S R and Sathyamurthy N 2008 *J. Phys. Chem.* **A112** 7699 (b) Elango M, Subramanian V and Sathyamurthy N 2008 *J. Phys. Chem.* **A112** 8107 (c) Elango M, Parthasarathi R, Subramanian V and Sathyamurthy N 2005 *J. Phys. Chem.* **A109** 8587
20. Turi L and Dannenberg J J 1994 *J. Am. Chem. Soc.* **116** 8714
21. Masunov A and Dannenberg J J 2000 *J. Phys. Chem.* **B104** 806
22. Turi L and Dannenberg J J 1996 *J. Phys. Chem.* **100** 9638
23. (a) Vijay D and Sastry G N 2010 *Chem. Phys. Lett.* **485** 235 (b) Vijay D, Zipse H and Sastry G N 2008 *J. Phys. Chem.* **B112** 8863 (c) Reddy A S, Vijay D, Sastry G M and Sastry G N 2006 *J. Phys. Chem.* **B110** 2479 (d) Reddy A S, Vijay D, Sastry G M and Sastry G N 2006 *J. Phys. Chem.* **B110** 10206
24. (a) Cabaleiro-Lago E M and Otero J R 2002 *J. Chem. Phys.* **117** 1621 (b) Guo H and Karplus M 1994 *J. Phys. Chem.* **98** 7104 (c) Kobko N, Paraskevas L, del Rio E and Dannenberg J J 2001 *J. Am. Chem. Soc.* **123** 4348 (d) Esrafilii M D, Behzadi H and Hadipour N L 2008 *Theor. Chem. Account.* **121** 135
25. (a) Kobko N and Dannenberg J J 2003 *J. Phys. Chem.* **A107** 10389 (b) Kobko N and Dannenberg J J 2003 *J. Phys. Chem.* **A107** 6688
26. Mahadevi A S, Neela Y I and Sastry G N 2011 *Phys. Chem. Chem. Phys.* **13** 15211
27. Boys S F and Bernardi F 1970 *Mol. Phys.* **19** 553
28. Frisch M J, Trucks G W, Schlegel H B, Scuseria G E, Robb M A, Cheeseman J R, Montgomery J A Jr, Vreven T, Kudin K N, Burant J C, Millam J M, Iyengar S S, Tomasi J, Barone V, Mennucci B, Cossi M, Scalmani G, Rega N, Petersson G A, Nakatsuji H, Hada M, Ehara M, Toyota K, Fukuda R, Hasegawa J, Ishida M, Nakajima T, Honda Y, Kitao O, Nakai H, Klene M, Li X, Knox J E, Hratchian H P, Cross J B, Bakken V, Adamo C, Jaramillo J, Gomperts R, Stratmann R E, Yazyev O, Austin A J, Cammi R, Pomelli C, Ochterski J W, Ayala P Y, Morokuma K, Voth G A, Salvador P, Dannenberg J J, Zakrzewski V G, Dapprich S, Daniels A D, Strain M C, Farkas O, Malick D K, Rabuck A D, Raghavachari K, Foresman J B, Ortiz J V, Cui Q, Baboul A G, Clifford S, Cioslowski J, Stefanov B B, Liu G, Liashenko A, Piskorz P, Komaromi I, Martin R L, Fox D J, Keith T, Al-Laham M A, Peng C Y, Nanayakkara A, Challacombe M, Gill P M W, Johnson B, Chen W, Wong M W, Gonzalez C and Pople J A 1998 *Gaussian 03, Revision E.01*, Gaussian, Inc., Pittsburgh, PA
29. (a) Bader R F W 1990 *Atoms in molecules: a quantum theory* (Clarendon Press) (b) AIM 2000 Biegler-Konig F, Schonbohm J, Derdau R, Bayles D and Bader R F W 2000 *Version 1* (Bielefeld, Germany) (c) Parthasarathi R, Subramanian V and Sathyamurthy N 2006 *J. Phys. Chem.* **A110** 3349